Ecological Indicators 188 (2026) 115018

Contents lists available at ScienceDirect

Ecological Indicators

journal homepage: www.elsevier.com/locate/ecolind

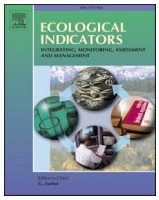

Exploring climate change exposure of the Mediterranean Sea through 3D climate velocity

Alessia Rizzi [a,b,*], Stefano Menegon [a,b], Marco Fianchini [c,b], Donata Melaku Canu [b,c], Elena Gissi [a,b]

[a] National Research Council, Institute of Marine Sciences CNR ISMAR, Venice, Italy
[b] National Biodiversity Future Center, Palermo, Italy
[c] National Institute of Oceanography and Applied Geophysics OGS, Trieste, Italy

ARTICLE INFO

Keywords:
Climate velocity
Climate analogues
Vertical climate change
Marine climate refugia
Mediterranean Sea
Marine spatial planning

ABSTRACT

Climate change is increasingly challenging the durability of marine conservation and spatial planning approaches that rely on contemporary climate baselines. In response, the identification and protection of climate refugia – areas expected to remain relatively stable under climate change – has emerged as a key strategy for climate-smart conservation. However, in marine systems, refugia are commonly delineated using surface conditions alone, overlooking the vertical structure of the ocean. Here, we assess climate change exposure across the entire Mediterranean Sea water column using an analogue-based climate velocity framework in three-dimensional space. We compared present (2006–2030) and near-future (2031–2055) temperature conditions using nine climate variables, constraining the search for climatic analogues within ecologically meaningful depth ranges. Projected temperature conditions shifted in three dimensions across most of the basin: 45.8% of the Mediterranean exhibited combined horizontal and vertical displacement of climate conditions, while an additional 13.4% showed predominantly vertical shifts, indicating that climate change does not operate solely through horizontal redistribution. The basin-wide mean three-dimensional climate velocity was 2.98 km yr^{-1}, with pronounced depth- and region-specific differences. Climate exposure was highest in the euphotic zone and in deep regions such as the Ionian Sea, whereas deeper biozones of the Western Mediterranean appeared comparatively more stable than those of the Eastern region. By integrating depth-resolved climate data within a fully three-dimensional framework, this study provides the first basin-scale assessment of climate velocity across the Mediterranean water column and offers a robust foundation for climate-smart conservation and planning.

1. Introduction

Climate change is profoundly altering marine ecosystems by driving shifts in species distributions and modifying patterns of occurrence (Pinsky et al., 2025; Pinsky et al., 2020). These changes disrupt community dynamics, reshape ecosystem structure, and affect ecosystem functioning and the services they provide (Doney et al., 2012; Pecl et al., 2017). As a result, the effectiveness of current conservation strategies, such as marine protected areas (MPAs), is expected to decline, as only a subset may be able to maintain the biodiversity they currently support under future conditions (Dobrowski et al., 2021; Kyprioti et al., 2021). In parallel, climate-driven redistribution of human activities may intensify spatial conflicts, underscoring the need for adaptive maritime spatial planning (MSP). Together, these pressures challenge existing conservation and management frameworks and underscore the need for climate-smart conservation – and particularly climate-smart MSP – to ensure that conservation objectives remain effective under future climate scenarios (Frazão Santos et al., 2024; Frazão Santos et al., 2020; Gissi et al., 2019; Solidoro et al., 2022).

To operationalise climate-smart conservation and MSP, increasing emphasis has been placed on identifying and protecting climate refugia, which are considered key targets for conservation (Brito-Morales et al., 2022; Buenafe et al., 2023; Doxa et al., 2022b). Climate refugia buffer species, populations, or ecosystems from climate change by maintaining relatively stable environmental conditions over time, allowing biodiversity to persist in place (Carroll et al., 2017; Loarie et al., 2009). They

* Corresponding author at: National Research Council, Institute of Marine Sciences CNR ISMAR, Venice, Italy.
E-mail addresses: alessiarizzi@cnr.it (A. Rizzi), stefano.menegon@cnr.it (S. Menegon), mfianchini@ogs.it (M. Fianchini), dcanu@ogs.it (D. Melaku Canu), elena.gissi@cnr.it (E. Gissi).

https://doi.org/10.1016/j.ecolind.2026.115018
Received 23 January 2026; Received in revised form 27 May 2026; Accepted 27 May 2026
Available online 4 June 2026

are often characterised by high environmental heterogeneity, offering a variety of microhabitats that facilitate persistence, movement, or adaptation, and have historically facilitated species survival during past climate fluctuations (Brown et al., 2022; Michalak et al., 2020).

Several approaches have been proposed to identify potential refugia, including metrics based on the ratio between temporal climate trends and spatial gradients (Burrows et al., 2014; Loarie et al., 2009), distances to future locations with similar climate conditions (Hamann et al., 2015; Kyprioti et al., 2021; Ordonez and Williams, 2013), changes in habitat suitability (Serra-Diaz et al., 2014); and projection of persistent suitable conditions (Carroll et al., 2015). Together, these methods capture different dimensions of how refugia may support biodiversity persistence under climate change.

Among these approaches, analogue-based climate velocity focuses on exposure to change by identifying areas that maintain stable climatic conditions between the present and the future (Kyprioti et al., 2021). It estimates the distance an organism would need to cover to reach future locations with climatic conditions similar to those of its current habitat; effectively tracking the displacement of climatic niches over time (Kyprioti et al., 2021; Queirós et al., 2021). Locations with nearby future climate analogues, or where conditions remain stable, are potential refugia, whereas areas with distant or no analogues are considered climate change hotspots. Although originally developed in terrestrial systems (Carroll et al., 2017; Haight and Hammill, 2020; Loarie et al., 2009), analogue-based climate velocity is increasingly applied in the marine realm to assess climate stability within conservation contexts (e.g., Brito-Morales et al., 2022; Doxa et al., 2022a; Kyprioti et al., 2021); And to identify disturbance refugia; where key physical; ecological; and sociocultural features may persist under climate stress (Morelli et al., 2016; Saunders et al., 2023).

To date, most marine applications of climate velocity have relied on sea surface temperature (SST), due to its ecological relevance, strong link with other biogeochemical variables, and the availability of high-resolution datasets (Brito-Morales et al., 2018; Sanz-Martín et al., 2024). However, many marine species respond to temperature shifts both horizontally and across depth (Poloczanska et al., 2016; Von Schuckmann et al., 2023), and suitable conditions may be tracked through relatively small vertical movements rather than large horizontal displacements (Gruenburg et al., 2025). Although most excess heat is absorbed in the upper ocean; warming also occurs at intermediate depths and deep layers; which together contribute to a substantial fraction of ocean heat-content increase (Cheng et al., 2016; Desbruyères et al., 2016; Von Schuckmann et al., 2023). As a result, SST-based analyses may provide an incomplete representation of climate change for depth-dwelling species (Brito-Morales et al., 2018); failing to capture subsurface thermal dynamics and vertical heterogeneity that are fundamental to three-dimensional marine environments (Radin and Nieves, 2024; Zhang et al., 2023). While some studies have incorporated depth by calculating horizontal climate velocity within stratified depth zones (e.g., Brito-Morales et al., 2020; Doxa et al., 2022a), these approaches often assume homogeneity within depth layers and overlook interactions between horizontal and vertical climate gradients.

In this study, we explore climate refugia across the vertical domain by computing three-dimensional analogue-based climate velocity – across latitude and longitude, depth, and time – throughout the Mediterranean Sea. This basin is a global climate change hotspot due to its semi-enclosed nature, steep environmental gradients, and accelerated warming trends (Adloff et al., 2015; Giorgi, 2006; Vargas-Yáñez et al., 2008), with spatially heterogeneous impacts driven by circulation patterns, bathymetry, and thermal structure (Reale et al., 2022). This is the first study to apply a fully 3D analogue-based climate velocity to the Mediterranean basin, providing a spatially explicit framework for integrating vertical and horizontal climate refugia into climate-smart ocean planning.

2. Materials and methods

2.1. Defining the 3D analogue-based climate velocity

Analogue-based climate velocity quantifies the distance to the closest location whose future climate is analogous to a location's current climate (Ordonez and Williams, 2013); divided by the time interval over which the change is evaluated. Unlike the original climate velocity metric based on local spatial gradients (Loarie et al., 2009); analogue-based approaches identify climatically similar locations across the entire study region (Brito-Morales et al., 2018; Carroll et al., 2015; Ordonez and Williams, 2013).

Here we extend analogue-based climate velocity into the vertical dimension (Fig. 1) by computing geographic distances in a projected metric space, combining longitude (X), latitude (Y), and depth (Z). This three-dimensional implementation enables the identification of climate analogues both horizontally and vertically throughout the water column.

2.2. Climate data

We applied the 3D analogue-based method to a depth-resolved temperature dataset covering the full Mediterranean water column. We used daily sea temperature data (2006–2055) simulated by the POLCOMS-ERSEM coupled model under the Representative Conservation Pathway (RCP) 8.5 scenario, obtained from the Copernicus Climate Data Store (C3S, CDS, 2020; Kay et al., 2020). The dataset has a horizontal resolution of $0.1^\circ \times 0.1^\circ$ (~11 km) and includes 43 irregularly spaced vertical layers from 0.5 to 5500 m depth (Table S1). RCP 8.5 scenario represents a high-emission "business-as-usual" pathway selected here as the most realistic baseline for near-term climate projections; given that current global emissions trajectories remain closely aligned with its projections (Schwalm et al., 2020). Lower emission scenarios, while desirable, presuppose mitigation efforts that have not yet materialised at the required scale.

The time series was divided into two 25-year periods representing contemporary (2006–2030) and near-future (2031–2055) conditions. For each period, we computed nine temperature-based bioclimatic variables (O'Donnell and Ignizio, 2012) and averaged them over time for each cell and depth layer. Variables included annual mean temperature; diurnal range; isothermality; temperature seasonality; maximum and minimum temperature; annual range; and mean temperature of the warmest and coldest quarters (Table S2). These variables are widely used in species distribution and climate-impact studies (de Jesus Almeida et al., 2025). All analyses were conducted in Python (v3.9.18); and the full workflow is publicly available (Rizzi et al., 2026a).

To reduce dimensionality and collinearity, and ensure comparability across variables with different units, we performed a Principal Component Analysis (PCA) on the combined present and future bioclimatic datasets. Variables were standardised prior to analysis. PCA structure and loadings were examined across the full water column and within four ecologically meaningful vertical biozones: euphotic (0–40 m), mesophotic (40–200 m), mesopelagic (200–1000 m), and bathy-abyssopelagic (>1000 m), following Rogers (2015) and Doxa et al. (2022a) (Table S2). Because the vertical structure and relative importance of bioclimatic variables differ among biozones (Figs. S1-S3), analogue-based climate velocity was stratified across depth domains. The first three principal components, explaining >95% of the total variance in each biozone (Fig. S1), were used for subsequent analyses.

2.3. 3D climate velocity computation

We calculated 3D climate velocity independently within each biozone using an analogue-based approach (Carroll et al., 2015; Kyprioti et al., 2021; Ordonez and Williams, 2013). Climate similarity between

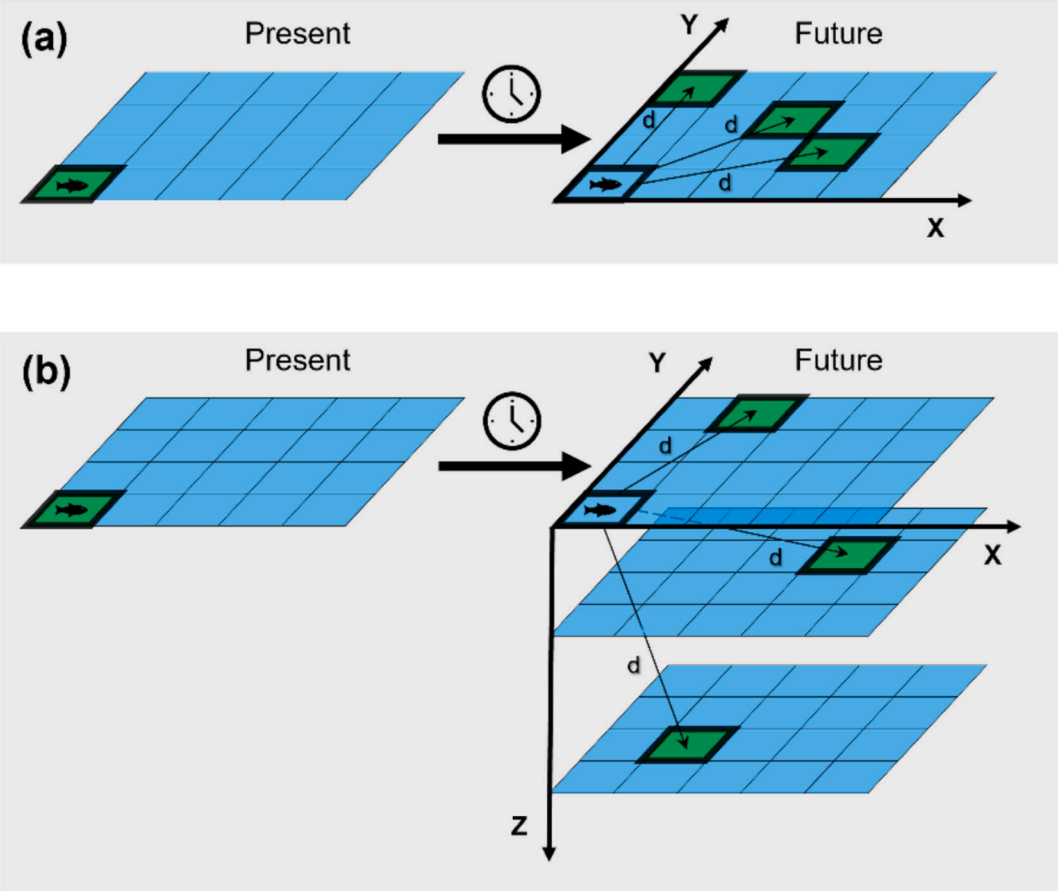

Fig. 1. Conceptual illustration of analogue-based climate velocity in two and three dimensions.
Present-day (left) and future (right) climate conditions are shown as grids. A focal cell (green, species icon) represents suitable climate, with arrows indicating the distance (d) required to track its future analogue. (a) 2D climate velocity: analogues search limited to the horizontal (X-Y) plane. (b) 3D climate velocity: analogue search extended to include the vertical dimension (X-Y-Z). (For interpretation of the references to colour in this figure legend, the reader is referred to the web version of this article.)

cells was quantified as Euclidean distance in PCA space. To identify valid climate analogues, we applied a continuous, distance-based similarity threshold calibrated through sensitivity analysis across a range of values (0.01–0.2 Euclidean distance units), jointly evaluating analogue displacement distances and the proportion of no analogue cells (Fig. S4). Excessively permissive thresholds make analogues trivially easy to find, compressing estimated velocities toward zero; conversely, overly restricted thresholds instead require near-identical PC values across cells, inflating the proportion of no analogue conditions (Hamann et al., 2015). Biozone-specific thresholds were therefore selected at the inflexion point of this trade-off; balancing spatial continuity and interpretability. Unlike previous implementations that rely on biome-derived cut-offs (Ordonez and Williams, 2013) or discretisation of climate space into predefined bins (Carroll et al., 2015; Kyprioti et al., 2021), this approach avoids imposing categorical ecological assumptions or artificial boundaries in multivariate climate space. Biozone-specific thresholds were selected to balance spatial continuity and interpretability.

Analogue searches were constrained to the same biozone as the focal cell, with the inclusion of one adjacent depth layer above and below to allow limited connectivity. Among all candidate analogues within the similarity threshold, the geographically nearest location in three-dimensional space (X, Y, Z) was selected as the future analogue (Carroll et al., 2015; Ordonez and Williams, 2013). Climate velocity was computed by dividing the geographic distance to the selected analogue by the 25-year time interval. The resulting climate velocity estimates are publicly available on Zenodo (Rizzi et al., 2026b).

2.4. Vertical and spatial analysis to identify refugia and hotspots

The 3D climate velocity vector was decomposed into horizontal (V_{xy}) and vertical (V_z) components. The horizontal component represents displacement in East-North space, while the vertical component is calculated as the depth difference between the focal and analogue locations, with positive values indicating upward shifts and negative values indicating downward shifts. Horizontal movement direction was derived from the V_{xy} vector and expressed as a compass bearing measured clockwise from North (0° = poleward, 180° = equatorward).

Climate velocity metrics were summarised by biozone using the mean, interquartile range (IQR), and maximum values (Max). Cells without a future analogue were classified as “no analogue”, while cells with zero horizontal and vertical displacement were classified as “no change”. Spatial patterns were analysed for the full Mediterranean basin and for individual basins defined following Manca et al. (2004; Fig. S5; Table S3).To further investigate depth-dependent differences; we calculated a normalised Euclidean dissimilarity index (Legendre and Legendre, 2012) between velocity fields across depth layers. This index quantifies the dissimilarity between full 2D grids at two depths, computed as a range-normalised Euclidean distance and aggregated across the horizontal grid for each depth, with higher values indicating greater dissimilarity.

Finally, we examined the 3D climate velocity vectors at the Mediterranean Sea surface (0.5 m), considering both their horizontal and vertical components. Separately, we also calculated a forward velocity constrained to the seafloor by limiting the search for analogues to

bottom grid cells; in this case, analogue coordinates were extracted in three dimensions (X, Y, Z), but velocity was computed solely from horizontal (X-Y) distances, without considering vertical displacement.

3. Results

3.1. Horizontal component of climate velocity

Under the extreme climate emissions scenario (RCP 8.5), the Mediterranean Sea was projected to experience substantial shifts in environmental conditions throughout the water column. The mean horizontal climate velocity was 2.98 km yr^{-1} (Table 1), corresponding to an average displacement of 74.5 km over the next 25 years, although values ranged from zero to peaks of 120 km yr^{-1}, particularly in the upper 30 m. Despite only 3.1% of points lacking future analogue, areas classified as 'no change' (both V_{xy} and $V_z = 0$) were scarce, representing just 11.9% of the Mediterranean. These rapid changes suggest that many marine species will need to track suitable thermal habitats across considerable distances within a few decades.

Among all vertical biozones, the euphotic zone was the most exposed to climate-induced temperature change, exhibiting the highest horizontal velocities and the most significant proportion of locations without future analogues (Table 1). Mean horizontal velocity reached 4.31 km yr^{-1}, with maxima up to 117.60 km yr^{-1}, primarily concentrated in areas close to the Strait of Gibraltar, along the Balearic Sea coasts, the northern Aegean, and along the coasts of Tunisia and Libya (Figs. 2–3). Moreover, 5.4% of locations lacked future analogues, forming pronounced clusters along the Tunisian coasts and in the Gulf of Lions and the Northern Adriatic Sea. In contrast, areas of no change represented 11.3% of the euphotic zone and were predominantly found in the Eastern Mediterranean.

Deeper biozones across the Mediterranean Sea were generally more stable than the euphotic zone, with mean horizontal velocities of 3.63, 1.69, and 2.49 km yr^{-1}, and no analogue proportions of 4.3%, 1.3%, and 3.9% in the mesophotic, mesopelagic, and bathyabyssopelagic biozones, respectively (Table 1). Nonetheless, the bathyabyssopelagic biozone exhibited marked climate exposure in some specific areas across the Mediterranean. We found widespread patches of elevated horizontal velocities alongside persistent no analogue areas, with values exceeding 10.00 km yr^{-1} and up to 6.9% no analogue (e.g., Ionian Sea; Fig. 2). This indicates that even the deepest layers are not uniformly stable and that climate-driven changes extend across the entire water column.

Finally, horizontal shifts toward future climate analogues showed no single dominant direction but were predominantly aligned along the East-West and North-South axes rather than along oblique directions. Each biozone exhibited distinct movement patterns, with no consistent direction emerging at the basin scale (Fig. 4). Comparing latitudinal and longitudinal components, shifts were generally more pronounced along the North-South axis than the East-West axis. Across all depth zones, northward and southward movements together accounted for approximately 40–50% of all displacement directions, whereas East-West shifts typically accounted for 25–30%. Moreover, except in the euphotic layer, where northward movement was slightly more frequent, southward shifts dominated the latitudinal component in deeper biozones. Nonetheless, eastward movement remained consistently represented across all depth ranges, contributing around 15–20% of total displacement directions.

3.2. Vertical component of climate velocity

Most of the Mediterranean Sea experienced climate shifts in both horizontal and vertical directions. Only 25.7% of points moved purely horizontally, whereas 45.8% underwent combined horizontal and vertical displacement, and 13.4% shifted exclusively along the vertical axis. Across the water column, mean vertical velocity was 1.77 m yr^{-1} (Table 1), but this average masked extreme local values, ranging from maxima of −70.00 m yr^{-1} near 1000 m depth to 140.00 m yr^{-1} at 4000 m. These results highlight that vertical displacements are widespread, emphasising that climate-driven changes cannot be fully captured by horizontal movement alone.

Vertical climate velocities displayed recurrently contrasting patterns across depth biozones. In the euphotic zone, movement was predominantly downward, with a mean velocity $V_z = -0.19$ m yr^{-1}, although some areas, particularly the Levantine Sea, remained nearly stable (Fig. 2). In the intermediate biozones of the mesopelagic, vertical shifts were highly variable, with positive, negative, and near-zero velocities frequently occurring in proximity. Upward-directed movement became more common in the deeper layers of these zones, while localised downward shifts persisted, reaching maxima around −40.00 m yr^{-1} (Fig. 3). In the bathyabyssopelagic zone, vertical velocities were generally strongly positive (mean ≈ 9 m yr^{-1}) and increased with depth, with the highest values occurring in the Ionian Sea. Nevertheless, downward movement still occurred in the upper part of this zone, with maxima below −50.00 m yr^{-1}. Notably, anomalous velocity patterns were frequently observed at the edges of adjacent biozones, likely reflecting artefacts where analogue conditions are more readily found in neighbouring zones than within the assigned one. Overall, these patterns reveal that vertical displacement is strongly depth-dependent and spatially heterogeneous, with opposing velocities often co-occurring throughout the water column.

3.3. Surface and bottom climate velocities and depth similarity

At the surface, climate velocity values only partially reflected the dynamics observed across the full water column (Fig. S6). The mean horizontal velocity at surface level was lower than that in the photic biozones ($V_{xy} = 2.59$ km yr^{-1}; Table 1), yet higher than in the pelagic zones, while the vertical component showed strongly negative values ($V_z = -0.47$ m yr^{-1}), indicating predominantly downward movement. The spatial distribution of both components closely mirrored that of the euphotic zone. However, horizontal velocities showed more widespread near-zero values, suggesting limited horizontal displacement in several

Table 1
Climate velocity metrics across Mediterranean depth domains.

	V_{xy} (km yr^{-1})	V_z (m yr^{-1})	No analogue area (%)	No change area (%)
Mediterranean Sea	2.98 ± 7.54	1.78 ± 8.06	3.1	11.9
Depth domains				
Surface layer (0.5 m depth)	2.59 ± 7.68	−0.48 ± 0.29	3.1	7.5
Euphotic zone	4.31 ± 10.01	−0.19 ± 0.29	5.8	8.7
Mesophotic zone	3.63 ± 8.25	0.34 ± 0.92	4.3	11.3
Mesopelagic zone	1.69 ± 4.11	2.89 ± 6.31	1.3	15.4
Bathyabyssopelagic zone	2.49 ± 4.39	9.07 ± 22.26	3.9	22.4
Seafloor	5.66 ± 9.57 (km yr^{-1})		18.1	16.4

Mean horizontal (V_{xy}, km yr-1) and vertical (V_z, m yr-1) climate velocities (± SD), percentage of cells with no future analogue, and percentage with no change are reported for the full water column, surface layer, four biozones, and seafloor. Biozone values are based on depth-restricted analogue searches; seafloor values represent bottom-constrained (2D) climate velocity.

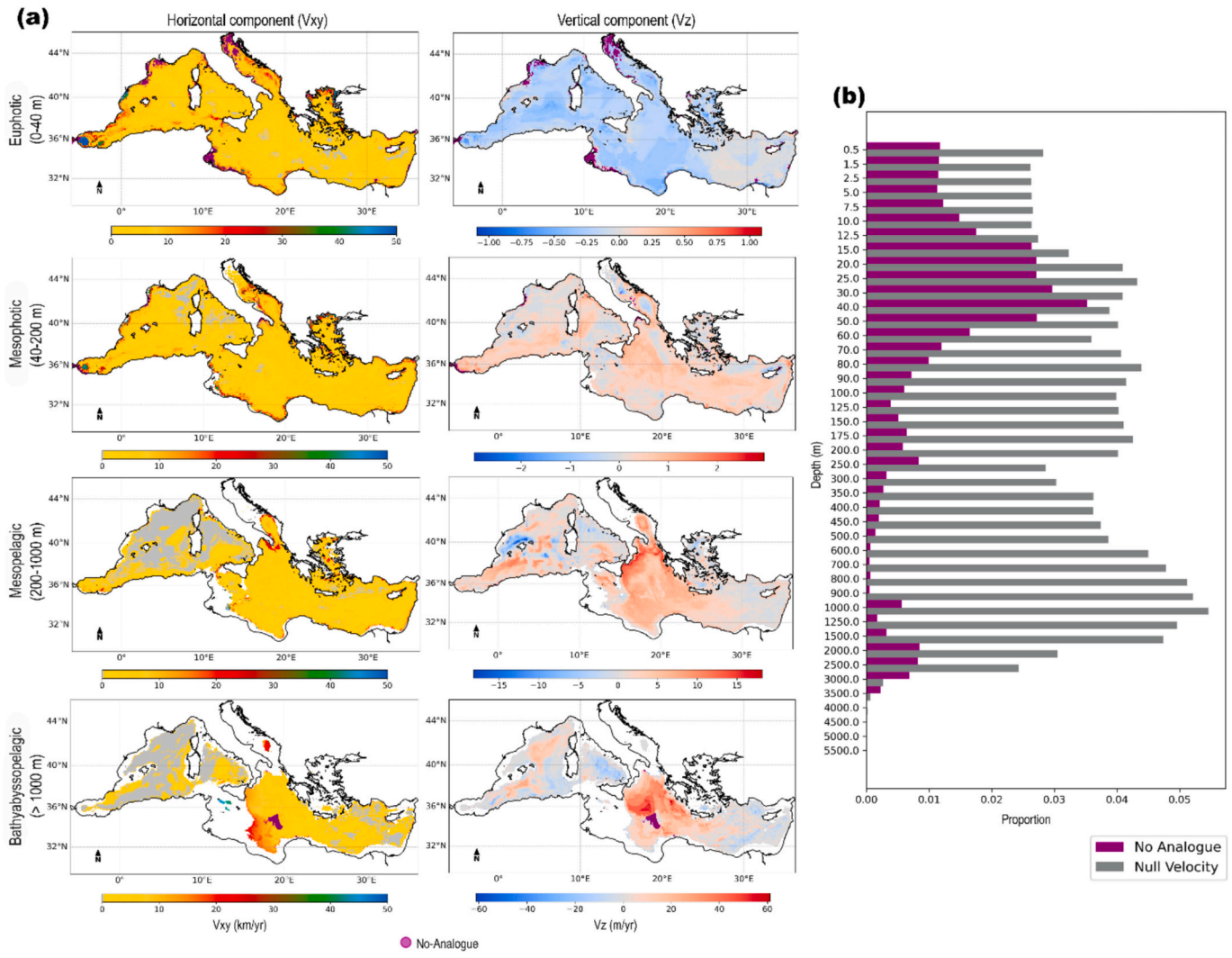

Fig. 2. Mean climate velocity (a) and analogue status (b) across Mediterranean biozones. (a) Mean horizontal (V_{xy}, km yr^{-1}) and vertical (V_z, m yr^{-1}) climate velocity for euphotic, mesophotic, mesopelagic, and bathyabyssopelagic zones. Horizontal velocities share a common colour scale across all biozones; vertical velocities use biozone-specific scaling to account for depth-layer spacing. No analogue points are shown where >50% of depth layers within a biozone lack a future analogue. (b) Proportion of points per depth with no analogue and no change (null velocity: $V_{xy} = V_z = 0$).

regions.

On the other hand, the seafloor appeared highly exposed to climate change, particularly in the shallow and deep portions of the Mediterranean. The overall mean bottom climate velocity (5.66 km yr^{-1}; Table 1) exceeded that of any biozone, with pronounced peaks in the deepest areas such as the southern Adriatic, Ionian Sea, and Strait of Sicily (Fig. S6). In contrast, the western Mediterranean and Levantine basins showed a larger proportion of cells with near-zero or moderate velocities (<5 km yr^{-1}). Locations without analogues were also relatively common (18.1%), occurring mainly along the coasts, across the entire Adriatic, and in deep offshore sectors such as the central Tyrrhenian and Ionian.

When examining depth similarity, horizontal and vertical velocities generally exhibited consistent patterns within each biozone, except between 15 and 75 m and in the deepest layers (Fig. 5). The dissimilarity index for horizontal velocity remained low (≤ 0.2) across most depths, except in the euphotic and mesophotic zones, where poor similarity (≈0.4) characterised the 15–75 m range. Another marked discontinuity occurred in the bathyabyssopelagic zone, where layers between 2000 and 3000 m displayed distinct behaviours, differing substantially both among themselves and from upper layers. Vertical velocity dissimilarities largely mirrored those of the horizontal component but were generally less pronounced, except below 3000 m, where values exceeded 0.4, indicating markedly different vertical velocities in the deepest layers. Overall, these results indicate that similarity in climate velocity across depths is structured rather than uniform, with specific depth ranges exhibiting distinct dynamics relative to adjacent layers.

3.4. Basin-scale patterns

Horizontal and vertical climate velocities differed markedly between the western and eastern Mediterranean, with the eastern basins generally more heterogeneous and exposed to climate-driven change than western basins.

Western basins (Provencal, Tyrrhenian, Alboran-Algerian, and Strait of Sicily) were generally more stable, particularly below the euphotic zone (Figs. S9, S12-S14). High horizontal velocities and concentrations of no-analogue areas were mainly confined to coastal sectors in the euphotic and mesophotic zones, while deeper biozones displayed mostly near-zero horizontal velocities (<2.00 km yr^{-1}; Table 2). Vertical velocities were generally modest, and a substantial proportion of points showed null climate velocity. Across most basins, more than 6.1% of areas exhibited no change at all depths, with this proportion increasing to 20–40% in deeper biozones. The Tyrrhenian was the main exception,

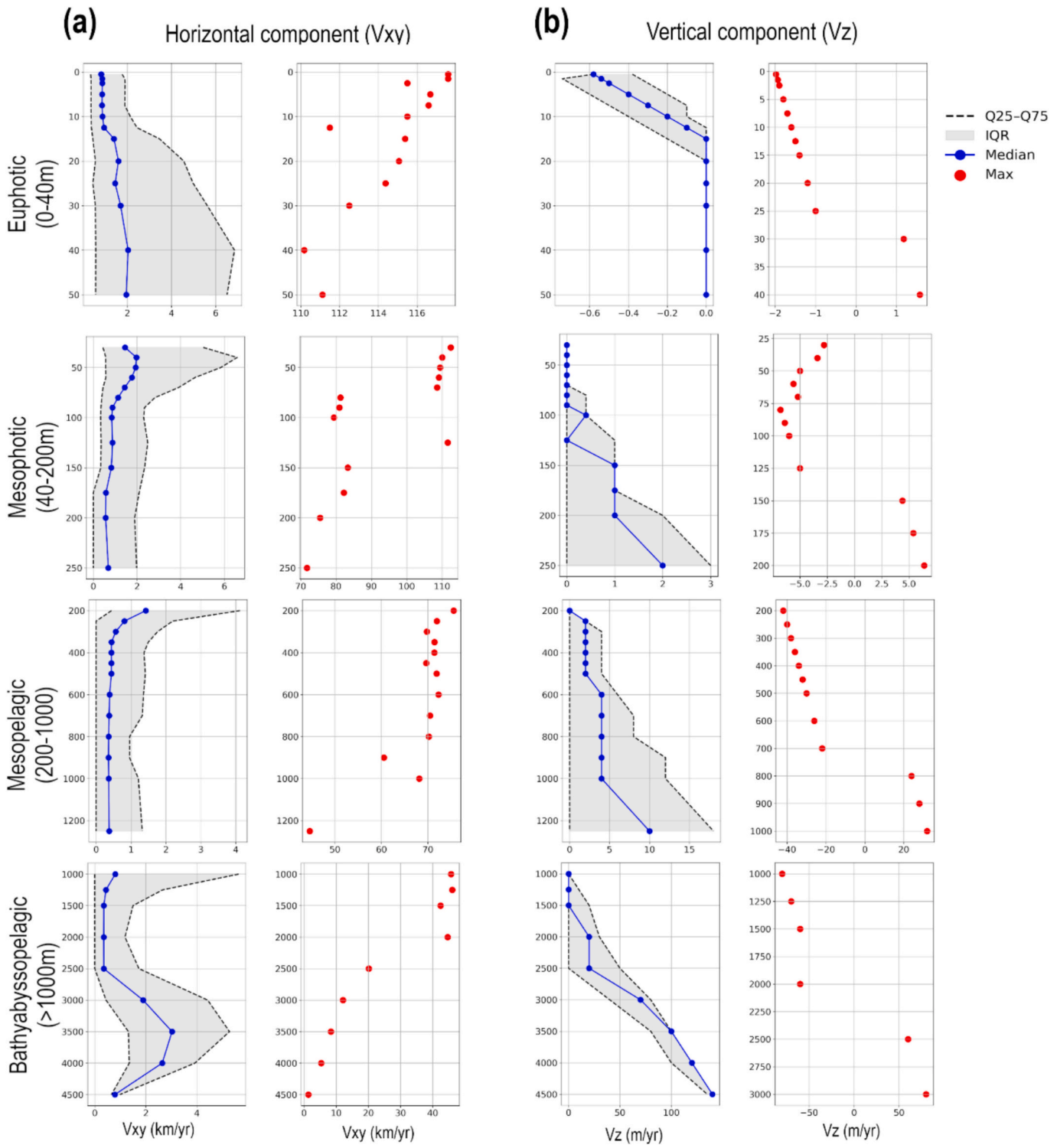

Fig. 3. Depth profiles of horizontal (V_{xy}) and vertical (V_z) climate velocity across Mediterranean biozones, showing median and maximum velocities for V_{xy} (a) and V_z (b). Median profiles includeinterquartile range; maximum profiles report the highest velocity per depth layer.

displaying consistently lower percentages across all depths. Downward-directed vertical velocities persisted in deeper areas, particularly in the bathyabyssopelagic Strait of Sicily and Tyrrhenian (means below −4.1 m yr^{-}), but concentration of negative means was also visible in the Balearic Sea. The rest of the areas showed near-zero or upward-directed velocities, with the highest peaks in the Ionian Sea at mesopelagic and bathyabyssopelagic levels. Overall, these features indicate that western basins are generally stable, with exposure restricted mainly to shallow coastal sectors.

Eastern basins were more heterogeneous. The Levantine Sea was the most stable, exhibiting low horizontal and vertical velocities throughout the water column and a higher proportion of no change cells than points without analogues (Table 2; Fig. S11). The Aegean exhibited contrasting patterns between horizontal and vertical components: horizontal velocity was higher in the euphotic zone (3.88 km yr^{-1}) and lower in deeper biozones (reaching 1.3 km yr^{-1} in the bathyabyssopelagic),

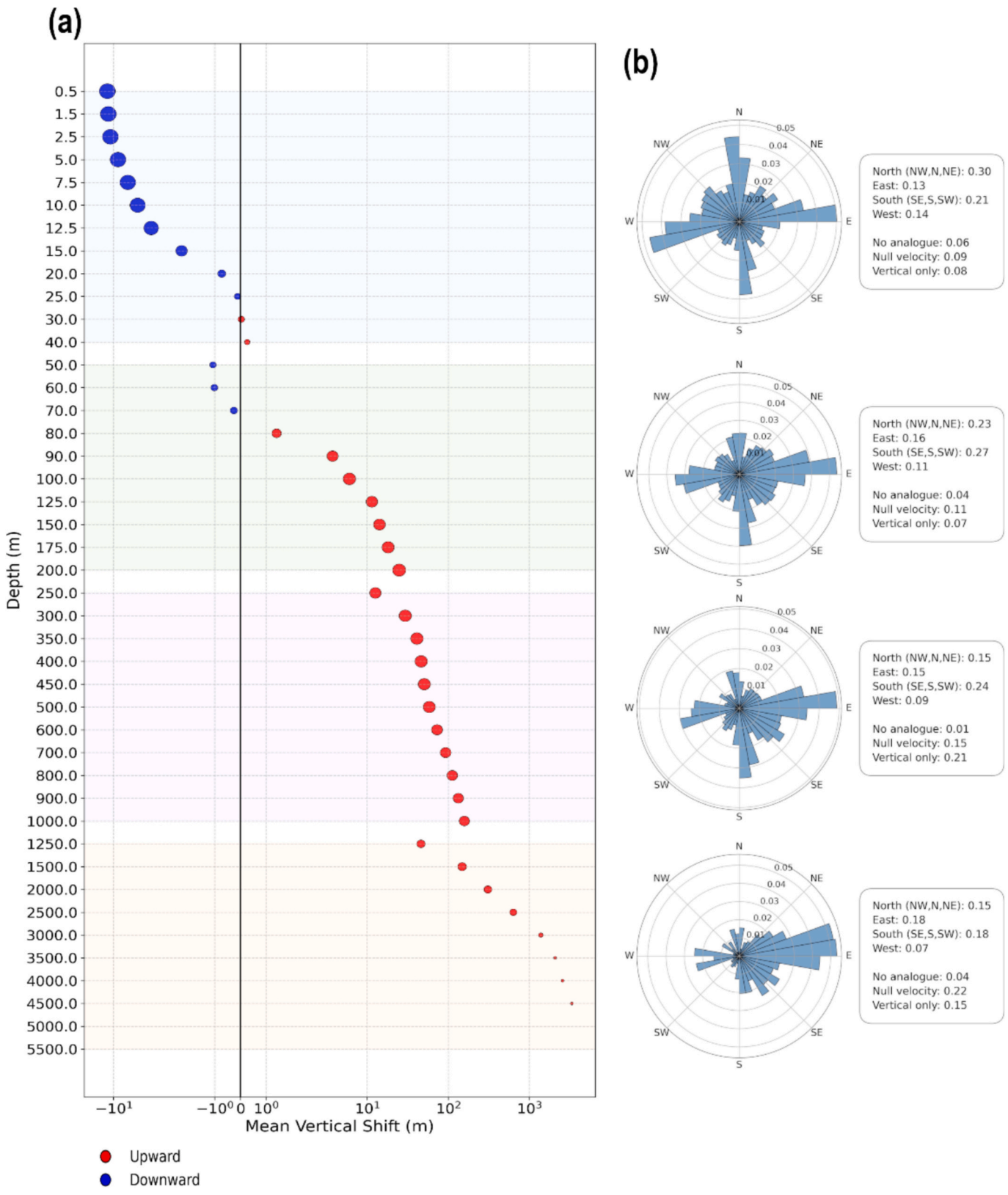

Fig. 4. Vertical (a) and horizontal (b) directions of climate-driven movement across Mediterranean biozones. (a) Mean vertical shifts per depth layer, with dot size reflecting the proportion of contributing points; logarithmic scale to accommodate depth-dependent spacing. (b) Rose diagrams of horizontal movement direction (0° = North), showing the proportion of points per direction, with summary fractions for cardinal sectors, no analogue, null horizontal velocity, and vertical-only shift. (For interpretation of the references to colour in this figure legend, the reader is referred to the web version of this article.)

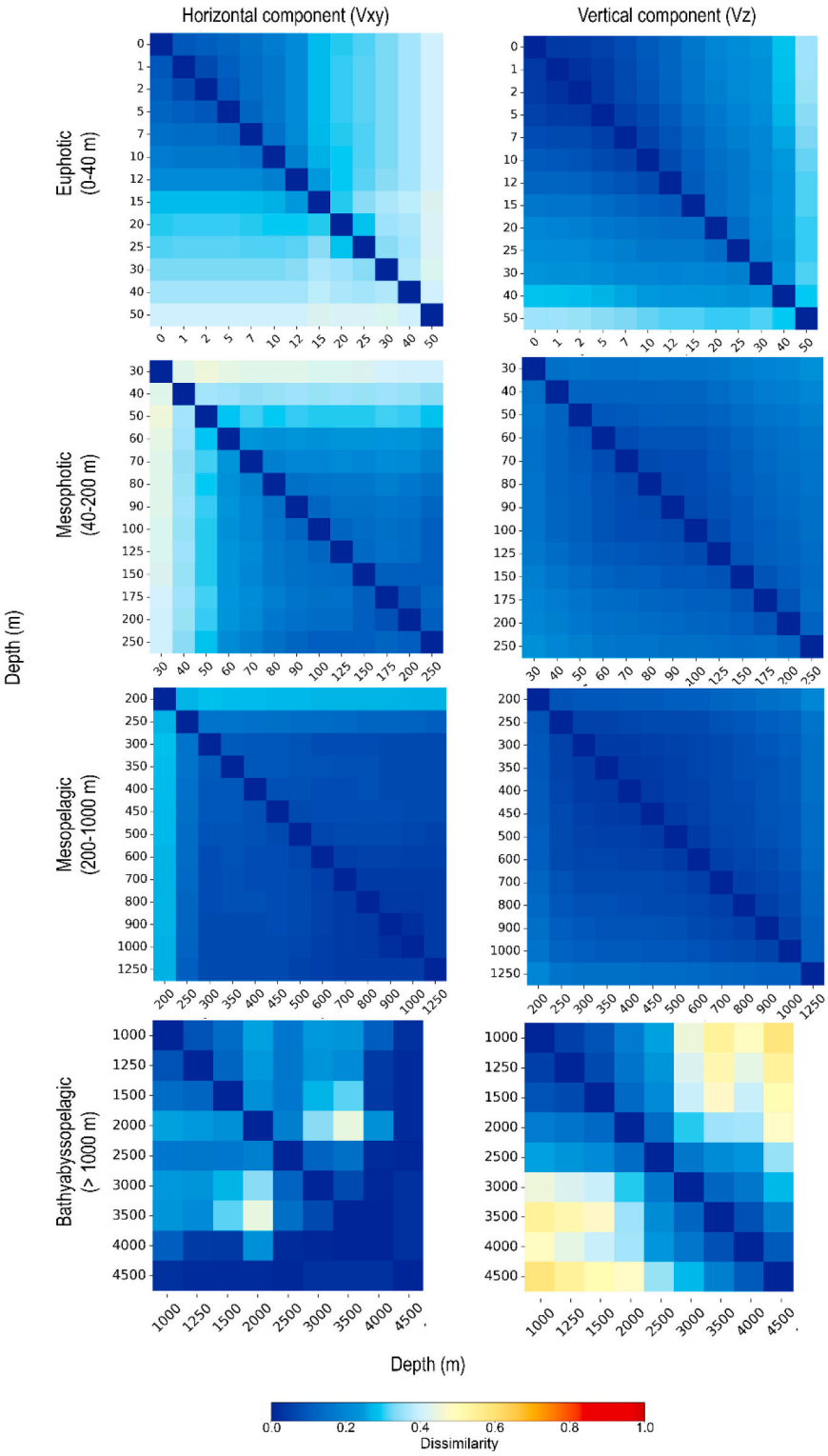

Fig. 5. Depth-layer dissimilarity of climate velocity within Mediterranean biozones. Heatmaps show pairwise dissimilarity between depth layers for horizontal (V_{xy}) and vertical (V_z) velocity. Values are normalised from 0 (identical) to 1 (maximal dissimilarity.

whereas vertical velocity shifted from slightly negative at the surface to strongly positive in the deepest layers (up to 10.2 m yr^{-1}). The Ionian Sea displayed a similar vertical trend, with negative values in the upper water column and positive values in deeper layers, while horizontal velocity was lower in intermediate zones but higher in the bathyabyssopelagic (6.50 km yr^{-1}), accompanied by clusters of no analogue points in these deeper layers (Fig. S10).

Among all basins, the Adriatic was the most exposed, showing high horizontal velocities in the photic zones (7.76 and 7.09 km yr^{-1} for euphotic and mesophotic zones, respectively; Table 2), and moderately lower values in pelagic zones (4.61 and 4.79 km yr^{-1} for mesopelagic and bathyabyssopelagic, respectively). The vertical component was negative in the euphotic zone, positive in the mesophotic zone, and strongly negative in the deepest zone. This basin also exhibited the most

Table 2
Climate velocity metrics by Mediterranean basin and biozone.

	Western Mediterranean				*Eastern Mediterranean*			
	Alboran-Algerian	Provencal	Sicily Strait	Tyrrhenian	Adriatic	Aegean	Ionian	Levantine
				Euphotic Zone				
V_{xy} (km yr^{-1})	6.66 ± 12.41	4.01 ± 7.6	4.52 ± 9.25	3.07 ± 6.65	7.76 ± 10.57	3.88 ± 10.89	3.02 ± 7.22	2.72 ± 7.64
V_z (m yr^{-1})	−0.24 ± 0.3	−0.22 ± 0.28	−0.23 ± 0.32	−0.23 ± 0.26	−0.22 ± 0.28	−0.13 ± 0.28	−0.25 ± 0.31	−0.03 ± 0.2
no analogue area (%)	23.8	2.2	6.5	1.9	4.5	8.8	6.3	2.7
no change area (%)	1.5	18.1	2.0	3.3	21.6	3.9	5.0	9.5
Mesophotic Zone								
V_{xy} (km yr^{-1})	4.2 ± 9.62	2.14 ± 6.05	2.65 ± 7.38	1.38 ± 4.59	7.09 ± 10.79	3.68 ± 8.86	3.8 ± 6.73	3.8 ± 8.12
V_z (m yr^{-1})	0.35 ± 0.87	0.2 ± 0.78	0.18 ± 0.87	0.29 ± 0.88	0.3 ± 1.16	0.36 ± 0.91	0.47 ± 0.96	0.35 ± 0.95
no analogue area (%)	11.2	3.1	6.2	2.5	5.1	4.9	2.9	2.1
no change area (%)	6.8	9.4	7.2	6.1	6.5	28.7	15.1	23.0
Mesopelagic Zone								
V_{xy} (km yr^{-1})	0.63 ± 2.72	0.23 ± 1.25	1.61 ± 4.95	0.61 ± 2.44	4.61 ± 6.71	1.52 ± 4.62	2.86 ± 3.85	1.89 ± 4.89
V_z (m yr^{-1})	1.8 ± 7.61	0.51 ± 6.89	2.28 ± 6.75	0.81 ± 6.38	3.92 ± 6.57	2.76 ± 4.46	6.38 ± 6.74	0.73 ± 2.95
no analogue area (%)	2.7	2.5	1.6	0.6	1.4	0.3	2.5	0.2
no change area (%)	13.1	6.4	22.5	1.5	13.6	43.7	14.7	27.3
Bathyabyssopelagic Zone								
V_{xy} (km yr^{-1})	0.29 ± 0.87	0.16 ± 0.66	2.02 ± 7.59	0.58 ± 1.57	4.79 ± 8.45	1.13 ± 2.07	6.49 ± 4.96	0.92 ± 2.47
V_z (m yr^{-1})	1.72 ± 13.51	4.33 ± 12.21	−4.13 ± 12.88	−5.31 ± 14.09	−5.19 ± 12.9	10.15 ± 16.34	24.96 ± 27.98	0.21 ± 12.73
no analogue area (%)	10.6	2.1	0.2	8.2	2.2	0.2	6.9	4.9
no change area (%)	32.1	9.4	42.8	0.5	29.0	49.5	16.3	31.5

Mean horizontal (V_{xy}, km yr^{-1}) and vertical (V_z, m yr^{-1}) climate velocity (± SD), percentage of cells with no future analogue, and percentage with no change are reported for each Mediterranean basin and biozone.

significant proportion of no analogue points across the water column (up to 21.6% in the euphotic; Fig. S7), while no change cells remained present (around 29.0% in the bathyabyssopelagic).

Depth-dependent vertical shifts in climate conditions further highlighted regional differentiation. Negative velocities dominated in the euphotic zone of nearly all basins, whereas positive velocities became increasingly frequent in the mesophotic and mesopelagic zones, particularly in the Adriatic, Aegean, and Ionian (Fig. S7). In the deepest biozone, upward displacements were dominant in some areas (Ionian), while other basins, such as the Tyrrhenian, Strait of Sicily, and Adriatic, exhibited negative downward-directed velocities. These results reveal a complex interplay among basin geography, depth, and climate exposure, with eastern basins exhibiting more heterogeneous and pronounced vertical and horizontal shifts than western Mediterranean basins.

4. Discussion

This study provides the first fully three-dimensional climate velocity assessment for the Mediterranean Sea, highlighting the importance of depth-resolved analyses for understanding climate-driven habitat change. While most existing assessments rely on sea surface temperature, our results show that present-day climatic conditions are projected to shift in three dimensions, reinforcing evidence that horizontal climate velocity alone provides an incomplete representation of marine climate change (Gruenburg et al., 2025). The three-dimensional framework revealed pronounced differences in climate exposure across Mediterranean biozones: surface patterns were broadly consistent across the basin, whereas deeper zones in the western Mediterranean remained comparatively stable and eastern basins exhibited higher velocities. Such depth- and region-specific patterns cannot be captured by surface- or bottom-only approaches, underscoring the need for conservation strategies tailored to both basin and depth range to protect shallow and deep-water refugia.

We observed marked regional differentiation between the Western and Eastern Mediterranean, reflecting basin geometry, circulation, and depth-dependent heat redistribution (Adloff et al., 2015). In the west; the euphotic zone showed high exposure; while deeper zones exhibited lower climate velocities; consistent with the moderating influence of Atlantic inflow through the Strait of Gibraltar (Kubin et al., 2023; Schroeder et al., 2016). However, some western basins, notably the Alboran-Algerian and Tyrrhenian, combined relatively low velocities with disproportionately high no analogue proportion, indicating that limited climate displacement does not necessarily imply accessible future conditions. In contrast, the Eastern Mediterranean showed more heterogeneous patterns: surface layers were generally less exposed, but deeper regions displayed elevated velocities, consistent with global analyses showing high climate velocity in deep marine environments (Brito-Morales et al., 2020). The Levantine basin exhibited relatively low exposure throughout the water column; possibly because this basin has already experienced progressive warming and tropicalization in recent decades (El-Geziry, 2021; Pastor et al., 2020; Pisano et al., 2020), with much of the climate shift projected elsewhere having already occurred. The Adriatic Sea maintained the highest velocities and relatively high no analogue proportions consistently across the entire water column, consistent with its limited water volume, restricted exchange, and strong atmospheric forcing (Da Costa et al., 2024; Moulin et al., 2024; Terzić et al., 2025). Instead, the Ionian emerged as the most exposed basin in the bathyabyssopelagic with the highest horizontal velocities and elevated no analogue proportions at depth. Overall, high climate velocities were generally accompanied by high no analogue proportions across basins and biozones, and vice versa, suggesting that both metrics consistently reflect the same underlying gradient of climate exposure, with notable exceptions in the deeper layers of some western basins.

Across the vertical domain, the euphotic zone emerged as the most exposed biozone, exhibiting the highest climate velocities, partially driven by pronounced peaks in the uppermost layers (≈120 km yr^{-1} within the first 10 m). This pattern aligns with projected warming, which is strongest at the surface and decreases with depth due to greater thermal inertia of subsurface waters (Cheng et al., 2016; Parras-Berrocal et al., 2023). As a result, future climate analogues for euphotic conditions were predominantly located at greater depths, reflected by consistently negative vertical climate velocity. In shallow coastal areas, where downward movement is constrained by bathymetry (Jorda et al.,

2019), clusters of no analogue locations indicate the local loss of viable future conditions. Together, these results highlight subsurface waters as potential vertical thermal refugia for surface-associated communities and emphasise the importance of explicitly accounting for depth in conservation planning.

In contrast, the deepest portions of the Mediterranean also emerged as potential hotspots of climate-driven change, exhibiting high horizontal and vertical climate velocities. Although deep-sea environments have long been considered thermally stable (Levin and Le Bris, 2015); modelling studies (Adloff et al., 2015; Reale et al., 2022; Solidoro et al., 2022) and our results indicate that even modest temperature increases can translate into substantial climatic displacement where horizontal gradients are weak (Brito-Morales et al., 2020; Levin and Le Bris, 2015). High horizontal velocities observed in deep regions such as the Ionian Sea, the Strait of Sicily, and the Southern Adriatic reflect the large spatial displacements required to locate future climate analogues under these conditions (Brito-Morales et al., 2020). Unlike the euphotic zone, where high mean velocities partly reflect concentrated extreme values in the shallowest depths, elevated means in the deepest biozone reflect a broader prevalence of sustained high velocities across much of the domain. These findings highlight that deep Mediterranean environments are not climatically inert but can experience substantial exposure driven by the interaction of horizontal and vertical climate gradients.

Vertical climate velocity in deeper biozones showed marked directional variability, with coexistence of downward-, upward-, and null shifts, indicating that climate responses are not transferable across depths. Downward-directed shifts reflect the pervasive vertical temperature gradient and are consistent with documented biological responses to upper-ocean warming (Chaikin et al., 2022; Poloczanska et al., 2016), potentially reinforced in the western basins by colder intermediate waters associated with the Atlantic inflow (Kubin et al., 2023). Null vertical velocities likely reflect recent changes in stratification that have reduced vertical thermal gradients; particularly in the Eastern Mediterranean (Artale et al., 2018). Upward-directed shifts; especially below 1000 m; may be linked to deep waters homogenisation and density-driven processes that locally weaken or invert vertical temperature gradients (Artale et al., 2018; Schroeder et al., 2016), and are consistent with observed upward depth shifts in some taxa (Chaikin et al., 2022; Chaikin and Belmaker, 2023; Sanz-Martín et al., 2024).

Climate analogues for surface conditions were most frequently found between 25 and 75 m depth, overlapping broadly with the mesophotic zone (Castellan et al., 2022). While mesophotic ecosystems are often considered potential climate refugia due to thermal buffering (Cerrano et al., 2019; Pichot et al., 2025), our results indicate a more nuanced role. Mesophotic depths acted as convergence zones for climate analogues from adjacent biozones, consistent with a vertical buffering effect (Cerrano et al., 2019); but also exhibited high climate velocities; frequent no analogue conditions; and patchy warming trajectory (de la Maza et al., 2024). This dual role suggests that mesophotic ecosystems may function as transient refugia for vertically-shifting species while remaining highly exposed themselves, challenging the assumption that they represent consistently stable climate refugia.

Horizontal climate velocity exhibited pronounced directional heterogeneity across depth and basins. While the euphotic zone showed predominantly northward shifts, consistent with surface warming trends (Rhein et al., 2013); deeper biozones displayed multidirectional movement (Brito-Morales et al., 2020); with a prevalence of counter-poleward and eastward components. This contrasts with the hypothesis of the Mediterranean Sea as an ecological cul-de-sac (Ben Rais Lasram et al., 2010) and suggests that suitable future conditions may also be accessed through equatorward or eastward shifts; potentially in combination with vertical redistribution (Sanz-Martín et al., 2024). These results highlight the importance of bathymetric structure and three-dimensional habitat availability in shaping climate-driven movement pathways.

Several methodological limitations should be acknowledged. Our analysis is based on static comparison of present and future temperature conditions and does not explicitly account for ocean dynamics, which strongly influence heat redistribution within the Mediterranean water column (Artale et al., 2018; Pisano et al., 2020). Nevertheless, approaches restricted to the surface or seafloor provide an overly simplified representation of climate change, as they neglect vertical pathways of climate tracking and may misidentify climate refugia. Despite not explicitly resolving circulation, a three-dimensional framework therefore offers a more realistic depiction of climate exposure in marine environments than surface- or bottom-restricted approaches.

The use of a single climate model simulation also represents an important limitation, as it does not sample the structural uncertainty associated with alternative model formulations, forcings, downscaling strategies, and scenario designs (Freer et al., 2018). The model used; POLCOMS-ERSEM; is a state-of-the-art regional model for basin-scale Mediterranean climate analysis. It has been evaluated against satellite and in situ observation (Kay et al., 2018; Ramirez-Romero et al., 2020), and its temperature trend agrees with the Med-CORDEX ensemble, where water column warming emerges as a robust feature across models (Soto-Navarro et al., 2020). However; local structures are strongly model-dependent; and no clear consensus emerges for key regional processes. The spatial resolution of POLCOMS-ERSEM is also not adequate to fully resolve submesoscale processes; particularly in regions such as the Adriatic; where a higher-resolution and ocean-atmosphere coupled configuration can improve the realism of dense-water formation; although important biases may still remain (Dunić et al., 2019). While these limitations should be transparently communicated, POLCOMS-ERSEM remains appropriate for identifying first-order, basin-scale patterns of climate exposure, and as such, holds value as a representation of the best available knowledge in the Mediterranean.

In addition, analogue searches do not consider geographical or topographic barriers, potentially underestimating effective horizontal displacement where realistic pathways are constrained. Climate velocity metrics also assume unlimited dispersal and niche conservatism, assumptions that may not hold across taxa (Brito-Morales et al., 2018; Donelson et al.; 2019). In particular; high horizontal climate velocities detected in isolated deep regions may reflect the presence of climatic analogues in distant basins rather than locally accessible refugia; raising connectivity constraints that limit the ecological feasibility of such climate tracking. In such contexts; conservation strategies may need to move beyond the identification of climate refugia alone and also consider climate bright spots; where future environmental conditions may become favourable for some species despite not representing climatic stability sensu stricto (Queirós et al., 2021).

Furthermore, while the PCA-based aggregation of bioclimatic variables is designed to capture the full variance of projected temperature change, the resulting axes may not directly reflect biological importance. Notably, in this study, the variables contributing most to the principal components – including maximum temperature of the warmest month, minimum temperature of the coldest month, and mean temperatures of the warmest and coldest quarters – are those related to thermal extremes, which are particularly relevant for predicting species range shifts and assessing abrupt climate changes (Germain and Lutz, 2020; Maxwell et al., 2019).

To mitigate some of these limitations, we divided the water column into four ecologically meaningful biozones, limiting unrealistic vertical jumps, and accounting for key ecological constraints such as light availability. This framework is inherently flexible and can be tailored to species- or taxon-specific depth ranges, allowing climate-analogue searches to be constrained within ecologically realistic vertical domains. The biozone-based approach also reduced inflation effects associated with uneven vertical resolution, although differences in layer spacing remain an inherent limitation of three-dimensional climate analyses. However, constraining analogue searches to discrete biozones inevitably introduces boundary artefacts, and patterns observed at biozone edges should be interpreted with caution, as they may vary with

the choice of buffer layers above and below the defined depth ranges. To mitigate such boundary artefacts, we extended each biozone for one layer beyond depth limits. Nevertheless, the division into distinct biozones is ecologically essential rather than merely methodological. Separating the euphotic zone from deeper layers ensures that projected shifts for light-dependent species remain within ecologically viable depth ranges, avoiding unrealistic migrations into dim-light environments. Similarly, distinguishing the mesophotic zone and deeper biozones confines analogue searches within depth ranges sharing similar physical characteristics, preserving the ecological coherence of the resulting velocity estimates.

Finally, while temperature is a primary driver of marine climate change and a powerful basis for climate velocity analyses (García Molinos et al., 2016); future applications should move toward multi-stressor frameworks incorporating additional variables such as pH; oxygen; or productivity (Brito-Morales et al., 2018; Bopp et al., 2013; Hu et al.; 2024). Such approaches would better capture the complexity of climate impacts on marine ecosystems and improve the identification of climate refugia for conservation and climate-smart MSP. Similarly; while RCP8.5 currently aligns well with observed climate trends (Schwalm et al., 2020), considering multiple emission scenarios would be valuable to explore how patterns of climate exposure vary under different hypotheses.

Overall, integrating the vertical dimension fundamentally reshapes the assessment of climate exposure and refugia in the Mediterranean Sea. Our three-dimensional analogue-based framework reveals that depth is not a uniform buffer against climate change but a dynamic axis along which exposure and stability vary across basins and biozones.

5. Conclusions

By extending analogue-based climate velocity into three dimensions for the first time at the Mediterranean basin scale, this study reveals that climate exposure varies substantially across the water column, with marked depth- and region-dependent differences. Thermal conditions shift simultaneously in horizontal and vertical directions across most of the basin, with the euphotic zone emerging as the most exposed and subsurface mesophotic waters playing a dual role – as a potential refuge for surface communities and hotspots of change for their own. Even bathyabyssopelagic depths show elevated exposure, particularly in the Ionian Sea and the Adriatic, challenging the assumption that deep-sea environments are climatically inert (Levin and Le Bris, 2015). Together, these results underscore that surface- or bottom-restricted assessments cannot capture the full complexity of climate exposure in three-dimensional marine environments.

These findings carry direct implications for climate-smart conservation and marine spatial planning. Incorporating depth-resolved climate dynamics into the design of marine protected areas and spatial management frameworks can improve the protection of climate refugia, ultimately supporting more resilient and adaptive ocean governance in a rapidly changing Mediterranean Sea. Future work should extend this framework to multi-stressor contexts and multiple emission scenarios and integrate species-specific depth constraints to maximise its operational relevance for conservation and spatial planning.

Authors contribution

A.R., E.G., and S.M. conceptualized and designed the study and the methodology; A.R., S.M. collected data, performed the analysis; E.G. supervised the study and secured funds; A.R. and E.G. wrote the first draft of the manuscript, and A.R. designed the figures; all authors (A.R., E.G., S.M., D·C, and M.F.) contributed to the final version of the article.

CRediT authorship contribution statement

Alessia Rizzi: Writing – original draft, Visualization, Methodology, Formal analysis, Data curation, Conceptualization. **Stefano Menegon:** Writing – review & editing, Methodology, Formal analysis, Data curation, Conceptualization. **Marco Fianchini:** Writing – review & editing. **Donata Melaku Canu:** Writing – review & editing. **Elena Gissi:** Writing – review & editing, Writing – original draft, Supervision, Methodology, Funding acquisition, Conceptualization.

Declaration of competing interest

The authors declare that they have no known competing financial interests or personal relationships that could have appeared to influence the work reported in this paper.

Acknowledgments

This research was funded by the Italian National Recovery and Resilience Plan (NRRP), Mission 4 Component 2 Investment 1.4 - Call for tender No. 3138 of 16 December 2021, rectified by Decree n.3175 of 18 December 2021 of Italian Ministry of University and Research funded by the European Union – NextGenerationEU; Award Number: Project code CN-00000033, Concession Decree No. 1034 of 17 June 2022 adopted by the Italian Ministry of University and Research, CUP B83C22002930006, Project title “National Biodiversity Future Center – NBFC". The authors acknowledge the use of ChatGPT (OpenAI) for language editing and sentence structure assistance. All scientific content, interpretations, and conclusions remain the sole responsibility of the authors.

Appendix A. Supplementary data

Supplementary data to this article can be found online at https://doi.org/10.1016/j.ecolind.2026.115018.

Data availability

The code supporting the findings of this study is publicly available on Zenodo at doi:https://doi.org/10.5281/zenodo.18340030. NetCDF files containing climate velocity estimates for each biozone and the full water column, and the georeferenced raster maps (GeoTIFF) of velocity estimates for each depth layer, are publicly available on Zenodo at doi: https://doi.org/10.5281/zenodo.19606779.

Raw input climate data are publicly available from the Copernicus Climate Data Store (CDS) and are subject to the licensing and terms of use of the original data providers.

References

Adloff, F., Somot, S., Sevault, F., Jordà, G., Aznar, R., Déqué, M., Herrmann, M., Marcos, M., Dubois, C., Padorno, E., Alvarez-Fanjul, E., Gomis, D., 2015. Mediterranean Sea response to climate change in an ensemble of twenty first century scenarios. Clim. Dyn. 45, 2775–2802. https://doi.org/10.1007/s00382-015-2507-3.

Artale, V., Falcini, F., Marullo, S., Bensi, M., Kokoszka, F., Iudicone, D., Rubino, A., 2018. Linking mixing processes and climate variability to the heat content distribution of the eastern Mediterranean abyss. Sci. Rep. 8, 11317. https://doi.org/10.1038/s41598-018-29343-4.

Ben Rais Lasram, F., Guilhaumon, F., Albouy, C., Somot, S., Thuiller, W., Mouillot, D., 2010. The Mediterranean Sea as a ‘cul-de-sac’ for endemic fishes facing climate change. Glob. Chang. Biol. 16, 3233–3245. https://doi.org/10.1111/j.1365-2486.2010.02224.x.

Bopp, L., Resplandy, L., Orr, J.C., Doney, S.C., Dunne, J.P., Gehlen, M., Halloran, P., Heinze, C., Ilyina, T., Séférian, R., Tjiputra, J., Vichi, M., 2013. Multiple stressors of ocean ecosystems in the 21st century: projections with CMIP5 models. Biogeosciences 10, 6225–6245. https://doi.org/10.5194/bg-10-6225-2013.

Brito-Morales, I., García Molinos, J., Schoeman, D.S., Burrows, M.T., Poloczanska, E.S., Brown, C.J., Ferrier, S., Harwood, T.D., Klein, C.J., McDonald-Madden, E., Moore, P. J., Pandolfi, J.M., Watson, J.E.M., Wenger, A.S., Richardson, A.J., 2018. Climate velocity can inform conservation in a warming world. Trends Ecol. Evol. 33, 441–457. https://doi.org/10.1016/j.tree.2018.03.009.

Brito-Morales, I., Schoeman, D.S., Molinos, J.G., Burrows, M.T., Klein, C.J., Arafeh-Dalmau, N., Kaschner, K., Garilao, C., Kesner-Reyes, K., Richardson, A.J., 2020. Climate velocity reveals increasing exposure of deep-ocean biodiversity to future

warming. Nat. Clim. Chang. 10, 576–581. https://doi.org/10.1038/s41558-020-0773-5.
Brito-Morales, I., Schoeman, D.S., Everett, J.D., Klein, C.J., Dunn, D.C., García Molinos, J., Burrows, M.T., Buenafe, K.C.V., Dominguez, R.M., Possingham, H.P., Richardson, A.J., 2022. Towards climate-smart, three-dimensional protected areas for biodiversity conservation in the high seas. Nat. Clim. Chang. 12, 402–407. https://doi.org/10.1038/s41558-022-01323-7.
Brown, S.C., Mellin, C., García Molinos, J., Lorenzen, E.D., Fordham, D.A., 2022. Faster Ocean warming threatens richest areas of marine biodiversity. Glob. Chang. Biol. 28, 5849–5858. https://doi.org/10.1111/gcb.16328.
Buenafe, K.C.V., Dunn, D.C., Everett, J.D., Brito-Morales, I., Schoeman, D.S., Hanson, J. O., Dabalà, A., Neubert, S., Cannicci, S., Kaschner, K., Richardson, A.J., 2023. A metric-based framework for climate-smart conservation planning. Ecol. Appl. 33, e2852. https://doi.org/10.1002/eap.2852.
Burrows, M.T., Schoeman, D.S., Richardson, A.J., Molinos, J.G., Hoffmann, A., Buckley, L.B., Moore, P.J., Brown, C.J., Bruno, J.F., Duarte, C.M., Halpern, B.S., Hoegh-Guldberg, O., Kappel, C.V., Kiessling, W., O'Connor, M.I., Pandolfi, J.M., Parmesan, C., Sydeman, W.J., Ferrier, S., Williams, K.J., Poloczanska, E.S., 2014. Geographical limits to species-range shifts are suggested by climate velocity. Nature 507, 492–495. https://doi.org/10.1038/nature12976.
Carroll, C., Lawler, J.J., Roberts, D.R., Hamann, A., 2015. Biotic and climatic velocity identify contrasting areas of vulnerability to climate change. PLoS One 10, e0140486. https://doi.org/10.1371/journal.pone.0140486.
Carroll, C., Roberts, D.R., Michalak, J.L., Lawler, J.J., Nielsen, S.E., Stralberg, D., Hamann, A., Mcrae, B.H., Wang, T., 2017. Scale-dependent complementarity of climatic velocity and environmental diversity for identifying priority areas for conservation under climate change. Glob. Chang. Biol. 23, 4508–4520. https://doi.org/10.1111/gcb.13679.
Castellan, G., Angeletti, L., Montagna, P., Taviani, M., 2022. Drawing the borders of the mesophotic zone of the Mediterranean Sea using satellite data. Sci. Rep. 12, 5585. https://doi.org/10.1038/s41598-022-09413-4.
Cerrano, C., Bastari, A., Calcinai, B., Di Camillo, C., Pica, D., Puce, S., Valisano, L., Torsani, F., 2019. Temperate mesophotic ecosystems: gaps and perspectives of an emerging conservation challenge for the Mediterranean Sea. Eur. Zool. J. 86, 370–388. https://doi.org/10.1080/24750263.2019.1677790.
Chaikin, S., Belmaker, J., 2023. Fish depth redistributions do not allow maintenance of abundance in a region of rapid change. Oikos, e09650. https://doi.org/10.1111/oik.09650.
Chaikin, S., Dubiner, S., Belmaker, J., 2022. Cold-water species deepen to escape warm water temperatures. Glob. Ecol. Biogeogr. 31, 75–88. https://doi.org/10.1111/geb.13414.
Cheng, L., Trenberth, K.E., Palmer, M.D., Zhu, J., Abraham, J.P., 2016. Observed and simulated full-depth ocean heat-content changes for 1970–2005. Ocean Sci. 12, 925–935. https://doi.org/10.5194/os-12-925-2016.
Copernicus Climate Change Service, Climate Data Store, 2020. Marine Biogeochemistry Data for the Northwest European Shelf and Mediterranean Sea from 2006 up to 2100 Derived from Climate Projections. https://doi.org/10.24381/cds.dcc9295c.
Da Costa, V.S., Alessandri, J., Verri, G., Mentaschi, L., Guerra, R., Pinardi, N., 2024. Marine climate indicators in the Adriatic Sea. Front. Clim. 6, 1449633. https://doi.org/10.3389/fclim.2024.1449633.
de Jesus Almeida, M., de Matos, M.R.B., dos Santos, J.G.F., 2025. Bioclimatic variables used in predictive Modeling: a literature review for the caatinga biome. J. Bioeng. Technol. Health 7, 43–49. https://doi.org/10.34178/jbth.v7iSuppl1.441.
de la Maza, L., Wieters, E.A., Beldade, R., Landaeta, M.F., Perez-Matus, A., Navarrete, S. A., 2024. Variability in oceanographic conditions affecting mesophotic ecosystems along the south eastern Pacific: latitudinal trends and potential for climate refugia. J. Mar. Syst. 245, 103999. https://doi.org/10.1016/j.jmarsys.2024.103999.
Desbruyères, D.G., Purkey, S.G., McDonagh, E.L., Johnson, G.C., King, B.A., 2016. Deep and abyssal ocean warming from 35 years of repeat hydrography. Geophys. Res. Lett. 43. https://doi.org/10.1002/2016GL070413.
Dobrowski, S.Z., Littlefield, C.E., Lyons, D.S., Hollenberg, C., Carroll, C., Parks, S.A., Abatzoglou, J.T., Hegewisch, K., Gage, J., 2021. Protected-area targets could be undermined by climate change-driven shifts in ecoregions and biomes. Commun. Earth Environ. 2, 198. https://doi.org/10.1038/s43247-021-00270-z.
Donelson, J.M., Sunday, J.M., Figueira, W.F., Gaitán-Espitia, J.D., Hobday, A.J., Johnson, C.R., Leis, J.M., Ling, S.D., Marshall, D., Pandolfi, J.M., Pecl, G., Rodgers, G.G., Booth, D.J., Munday, P.L., 2019. Understanding interactions between plasticity, adaptation and range shifts in response to marine environmental change. Philos. Trans. R. Soc. Lond. B Biol. Sci. 374, 20180186. https://doi.org/10.1098/rstb.2018.0186Jennifer.
Doney, S.C., Ruckelshaus, M., Emmett Duffy, J., Barry, J.P., Chan, F., English, C.A., Galindo, H.M., Grebmeier, J.M., Hollowed, A.B., Knowlton, N., Polovina, J., Rabalais, N.N., Sydeman, W.J., Talley, L.D., 2012. Climate change impacts on marine ecosystems. Annu. Rev. Mar. Sci. 4, 11–37. https://doi.org/10.1146/annurev-marine-041911-111611.
Doxa, A., Almpanidou, V., Katsanevakis, S., Queirós, A.M., Kaschner, K., Garilao, C., Kesner-Reyes, K., Mazaris, A.D., 2022a. 4D marine conservation networks: combining 3D prioritization of present and future biodiversity with climatic refugia. Glob. Chang. Biol. 28, 4577–4588. https://doi.org/10.1111/gcb.16268.
Doxa, A., Kamarianakis, Y., Mazaris, A.D., 2022b. Spatial heterogeneity and temporal stability characterize future climatic refugia in Mediterranean Europe. Glob. Chang. Biol. 28, 2413–2424. https://doi.org/10.1111/gcb.16072.
Dunić, N., Vilibić, I., Šepić, J., Mihanović, H., Sevault, F., Somot, S., Waldman, R., Nabat, P., Arsouze, T., Pennel, R., Jordà, G., Precali, R., 2019. Performance of multi-decadal ocean simulations in the Adriatic Sea. Ocean Model 134, 84–109. https://doi.org/10.1016/j.ocemod.2019.01.006.
El-Geziry, T.M., 2021. Long-term changes in sea surface temperature (SST) within the southern Levantine Basin. Acta Oceanol. Sin. 40, 27–33. https://doi.org/10.1007/s13131-021-1709-2.
Frazão Santos, C., Agardy, T., Andrade, F., Calado, H., Crowder, L.B., Ehler, C.N., García-Morales, S., Gissi, E., Halpern, B.S., Orbach, M.K., Pörtner, H.-O., Rosa, R., 2020. Integrating climate change in ocean planning. Nat. Sustainability 3, 505–516. https://doi.org/10.1038/s41893-020-0513-x.
Frazão Santos, C., Agardy, T., Crowder, L.B., Day, J.C., Pinsky, M.L., Himes-Cornell, A., Reimer, J.M., García-Morales, S., Bennett, N.J., Lombard, A.T., Calado, H., Scherer, M., Flannery, W., Wedding, L.M., Gissi, E., 2024. Key components of sustainable climate-smart ocean planning. Npj Ocean Sustain. 3, 10. https://doi.org/10.1038/s44183-024-00045-x.
Freer, J.J., Partridge, J.C., Tarling, G.A., Collins, M.A., Genner, M.J., 2018. Predicting ecological responses in a changing ocean: the effects of future climate uncertainty. Mar. Biol. 165, 7. https://doi.org/10.1007/s00227-017-3239-1.
García Molinos, J., Halpern, B.S., Schoeman, D.S., Brown, C.J., Kiessling, W., Moore, P.J., Pandolfi, J.M., Poloczanska, E.S., Richardson, A.J., Burrows, M.T., 2016. Climate velocity and the future global redistribution of marine biodiversity. Nat. Clim. Chang. 6, 83–88. https://doi.org/10.1038/nclimate2769.
Germain, S.J., Lutz, J.A., 2020. Climate extremes may be more important than climate means when predicting species range shifts. Clim. Chang. 163, 579–598. https://doi.org/10.1007/s10584-020-02868-2.
Giorgi, F., 2006. Climate change hot-spots. Geophys. Res. Lett. 33, 2006GL025734. https://doi.org/10.1029/2006GL025734.
Gissi, E., Fraschetti, S., Micheli, F., 2019. Incorporating change in marine spatial planning: a review. Environ. Sci. Pol. 92, 191–200. https://doi.org/10.1016/j.envsci.2018.12.002.
Gruenburg, L.K., Nye, J., Lwiza, K., Thorne, L., 2025. Vertical climate velocity adds a critical dimension to species shifts. Nat. Clim. Chang. 15, 656–664. https://doi.org/10.1038/s41558-025-02300-6.
Haight, J., Hammill, E., 2020. Protected areas as potential refugia for biodiversity under climatic change. Biol. Conserv. 241, 108258. https://doi.org/10.1016/j.biocon.2019.108258.
Hamann, A., Roberts, D.R., Barber, Q.E., Carroll, C., Nielsen, S.E., 2015. Velocity of climate change algorithms for guiding conservation and management. Glob. Chang. Biol. 21, 997–1004. https://doi.org/10.1111/gcb.12736.
Hu, N., Bourdeau, P.E., Hollander, J., 2024. Responses of marine trophic levels to the combined effects of ocean acidification and warming. Nat. Commun. 15, 3400. https://doi.org/10.1038/s41467-024-47563-3.
Jorda, G., Marbà, N., Bennett, S., Santana-Garcon, J., Agusti, S., Duarte, C.M., 2019. Ocean warming compresses the three-dimensional habitat of marine life. Nat. Ecol. Evol. 4, 109–114. https://doi.org/10.1038/s41559-019-1058-0.
Kay, S., Andersson, H., Catalan, I., Eilola, K., Jordà, G., Ramirez-Romero, E., Wehde, H., 2018. Projections of Physical and Biogeochemical Parameters and Habitat Indicators for European Seas, Including Synthesis of Sea Level Rise and Storminess.
Kay, S., Clark, J., Hall, A., Marsh, J., Fernandes, J., 2020. Marine Biogeochemistry Data for the Northwest European Shelf and Mediterranean Sea from 2006 up to 2100 Derived from Climate Projections. https://doi.org/10.24381/cds.dcc9295c.
Kubin, E., Menna, M., Mauri, E., Notarstefano, G., Mieruch, S., Poulain, P.-M., 2023. Heat content and temperature trends in the Mediterranean Sea as derived from Argo float data. Front. Mar. Sci. 10, 1271638. https://doi.org/10.3389/fmars.2023.1271638.
Kyprioti, A., Almpanidou, V., Chatzimentor, A., Katsanevakis, S., Mazaris, A.D., 2021. Is the current Mediterranean network of marine protected areas resilient to climate change? Sci. Total Environ. 792, 148397. https://doi.org/10.1016/j.scitotenv.2021.148397.
Legendre, P., Legendre, L., 2012. Numerical Ecology, Developments in Environmental Modelling. Elsevier Science.
Levin, L.A., Le Bris, N., 2015. The deep ocean under climate change. Science 350, 766–768. https://doi.org/10.1126/science.aad0126.
Loarie, S.R., Duffy, P.B., Hamilton, H., Asner, G.P., Field, C.B., Ackerly, D.D., 2009. The velocity of climate change. Nature 462, 1052–1055. https://doi.org/10.1038/nature08649.
Manca, B., Burca, M., Giorgetti, A., Coatanoan, C., Garcia, M.-J., Iona, A., 2004. Physical and biochemical averaged vertical profiles in the Mediterranean regions: an important tool to trace the climatology of water masses and to validate incoming data from operational oceanography. J. Mar. Syst. 48, 83–116. https://doi.org/10.1016/j.jmarsys.2003.11.025.
Maxwell, S.L., Butt, N., Maron, M., McAlpine, C.A., Chapman, S., Ullmann, A., Segan, D. B., Watson, J.E.M., 2019. Conservation implications of ecological responses to extreme weather and climate events. Divers. Distrib. 25, 613–625. https://doi.org/10.1111/ddi.12878.
Michalak, J.L., Stralberg, D., Cartwright, J.M., Lawler, J.J., 2020. Combining physical and species-based approaches improves refugia identification. Front. Ecol. Environ. 18, 254–260. https://doi.org/10.1002/fee.2207.
Morelli, T.L., Daly, C., Dobrowski, S.Z., Dulen, D.M., Ebersole, J.L., Jackson, S.T., Lundquist, J.D., Millar, C.I., Maher, S.P., Monahan, W.B., Nydick, K.R., Redmond, K. T., Sawyer, S.C., Stock, S., Beissinger, S.R., 2016. Managing climate change refugia for climate adaptation. PLoS One 11, e0159909. https://doi.org/10.1371/journal.pone.0159909.
Moulin, A., Mentaschi, L., Clementi, E., Verri, G., Mercogliano, P., 2024. Projections of the Adriatic wave conditions under climate changes. Front. Clim. 6, 1409237. https://doi.org/10.3389/fclim.2024.1409237.
O'Donnell, M.S., Ignizio, D.A., 2012. Data Series 691 - Bioclimatic Predictors for Supporting Ecological Applications in the Conterminous United States (Data Series), Data Series. U.S. Department of the Interior, U.S. Geological Survey.

Ordonez, A., Williams, J.W., 2013. Projected climate reshuffling based on multivariate climate-availability, climate-analog, and climate-velocity analyses: implications for community disaggregation. Clim. Chang. 119, 659–675. https://doi.org/10.1007/s10584-013-0752-1.

Parras-Berrocal, I.M., Vázquez, R., Cabos, W., Sein, D.V., Álvarez, O., Bruno, M., Izquierdo, A., 2023. Dense water formation in the eastern Mediterranean under a global warming scenario. Ocean Sci. 19, 941–952. https://doi.org/10.5194/os-19-941-2023.

Pastor, F., Valiente, J.A., Khodayar, S., 2020. A warming Mediterranean: 38 years of increasing sea surface temperature. Remote Sens. 12, 2687. https://doi.org/10.3390/rs12172687.

Pecl, G.T., Araújo, M.B., Bell, J.D., Blanchard, J., Bonebrake, T.C., Chen, I.-C., Clark, T. D., Colwell, R.K., Danielsen, F., Evengård, B., Falconi, L., Ferrier, S., Frusher, S., Garcia, R.A., Griffis, R.B., Hobday, A.J., Janion-Scheepers, C., Jarzyna, M.A., Jennings, S., Lenoir, J., Linnetved, H.I., Martin, V.Y., McCormack, P.C., McDonald, J., Mitchell, N.J., Mustonen, T., Pandolfi, J.M., Pettorelli, N., Popova, E., Robinson, S.A., Scheffers, B.R., Shaw, J.D., Sorte, C.J.B., Strugnell, J.M., Sunday, J. M., Tuanmu, M.-N., Vergés, A., Villanueva, C., Wernberg, T., Wapstra, E., Williams, S.E., 2017. Biodiversity redistribution under climate change: impacts on ecosystems and human well-being. Science 355. https://doi.org/10.1126/science.aai9214.

Pichot, F., Manel, S., Velez, L., Juhel, J.-B., Ballesta, L., Boissery, P., Bruno, M., Cancemi, M., Riutort, J., Schultz, M., Tomasi, N., Valentini, A., Holon, F., Adam, O., Deter, J., Mouillot, D., 2025. Mesophotic Protected Habitats as Refugia for the Most At-Risk Elasmobranch Species. https://doi.org/10.2139/ssrn.5151816.

Pinsky, M.L., Selden, R.L., Kitchel, Z.J., 2020. Climate-driven shifts in marine species ranges: scaling from organisms to communities. Annu. Rev. Mar. Sci. 12, 153–179. https://doi.org/10.1146/annurev-marine-010419-010916.

Pinsky, M.L., Hillebrand, H., Chase, J.M., Antão, L.H., Hirt, M.R., Brose, U., Burrows, M. T., Gauzens, B., Rosenbaum, B., Blowes, S.A., 2025. Warming and cooling catalyse widespread temporal turnover in biodiversity. Nature 638, 995–999. https://doi.org/10.1038/s41586-024-08456-z.

Pisano, A., Marullo, S., Artale, V., Falcini, F., Yang, C., Leonelli, F.E., Santoleri, R., Buongiorno Nardelli, B., 2020. New evidence of Mediterranean climate change and variability from sea surface temperature observations. Remote Sens. 12, 132. https://doi.org/10.3390/rs12010132.

Poloczanska, E.S., Burrows, M.T., Brown, C.J., García Molinos, J., Halpern, B.S., Hoegh-Guldberg, O., Kappel, C.V., Moore, P.J., Richardson, A.J., Schoeman, D.S., Sydeman, W.J., 2016. Responses of marine organisms to climate change across oceans. Front. Mar. Sci. 3. https://doi.org/10.3389/fmars.2016.00062.

Queirós, A.M., Talbot, E., Beaumont, N.J., Somerfield, P.J., Kay, S., Pascoe, C., Dedman, S., Fernandes, J.A., Jueterbock, A., Miller, P.I., Sailley, S.F., Sará, G., Carr, L.M., Austen, M.C., Widdicombe, S., Rilov, G., Levin, L.A., Hull, S.C., Walmsley, S.F., Nic Aonghusa, C., 2021. Bright spots as climate-smart marine spatial planning tools for conservation and blue growth. Glob. Chang. Biol. 27, 5514–5531. https://doi.org/10.1111/gcb.15827.

Radin, C., Nieves, V., 2024. Unveiling regional climate patterns through global Subsurface Ocean temperature data: an AI multi-layer analysis framework. Earth Syst. Environ. 8, 1673–1681. https://doi.org/10.1007/s41748-024-00409-w.

Ramirez-Romero, E., Jordà, G., Amores, A., Kay, S., Segura-Noguera, M., Macias, D.M., Maynou, F., Sabatés, A., Catalán, I.A., 2020. Assessment of the skill of coupled physical–biogeochemical models in the NW Mediterranean. Front. Mar. Sci. 7, 497. https://doi.org/10.3389/fmars.2020.00497.

Reale, M., Cossarini, G., Lazzari, P., Lovato, T., Bolzon, G., Masina, S., Solidoro, C., Salon, S., 2022. Acidification, deoxygenation, and nutrient and biomass declines in a warming Mediterranean Sea. Biogeosciences 19, 4035–4065. https://doi.org/10.5194/bg-19-4035-2022.

Rhein, M., Rintoul, S.R., Aoki, S., Campos, E., Chambers, D., Feely, R.A., Gulev, S., Johnson, G.C., Josey, S.A., Kostianoy, A., Mauritzen, C., Roemmich, D., Talley, L.D., Wang, F., 2013. Observations: Ocean. In: Climate Change 2013 – The Physical Science Basis: Working Group I Contribution to the Fifth Assessment Report of the Intergovernmental Panel on Climate Change. Cambridge University Press, Cambridge, pp. 255–316. https://doi.org/10.1017/CBO9781107415324.010.

Rizzi, A., Menegon, S., Gissi, E., 2026a. 3D-climate-change-velocity v01 [code]. Zenodo. https://doi.org/10.5281/zenodo.18340430.

Rizzi, A., Menegon, S., Gissi, E., 2026b. 3D climate velocity dataset, Mediterranean Sea [dataset]. Zenodo. https://doi.org/10.5281/zenodo.19606779.

Sanz-Martín, M., Hidalgo, M., Puerta, P., Molinos, J.G., Zamanillo, M., Brito-Morales, I., González-Irusta, J.M., Esteban, A., Punzón, A., García-Rodríguez, E., Vivas, M., López-López, L., 2024. Climate velocity drives unexpected southward patterns of species shifts in the Western Mediterranean Sea. Ecol. Indic. 160, 111741. https://doi.org/10.1016/j.ecolind.2024.111741.

Saunders, S.P., Grand, J., Bateman, B.L., Meek, M., Wilsey, C.B., Forstenhaeusler, N., Graham, E., Warren, R., Price, J., 2023. Integrating climate-change refugia into 30 by 30 conservation planning in North America. Front. Ecol. Environ. 21, 77–84. https://doi.org/10.1002/fee.2592.

Schroeder, K., Chiggiato, J., Bryden, H.L., Borghini, M., Ben Ismail, S., 2016. Abrupt climate shift in the Western Mediterranean Sea. Sci. Rep. 6, 23009. https://doi.org/10.1038/srep23009.

Schwalm, C.R., Glendon, S., Duffy, P.B., 2020. RCP8.5 tracks cumulative CO_2 emissions. Proc. Natl. Acad. Sci. 117, 19656–19657. https://doi.org/10.1073/pnas.2007117117.

Serra-Diaz, J.M., Franklin, J., Ninyerola, M., Davis, F.W., Syphard, A.D., Regan, H.M., Ikegami, M., 2014. Bioclimatic velocity: the pace of species exposure to climate change. Divers. Distrib. 20, 169–180. https://doi.org/10.1111/ddi.12131.

Solidoro, C., Cossarini, G., Lazzari, P., Galli, G., Bolzon, G., Somot, S., Salon, S., 2022. Modeling carbon budgets and acidification in the Mediterranean Sea ecosystem under contemporary and future climate. Front. Mar. Sci. 8, 781522. https://doi.org/10.3389/fmars.2021.781522.

Soto-Navarro, J., Jordá, G., Amores, A., Cabos, W., Somot, S., Sevault, F., Macías, D., Djurdjevic, V., Sannino, G., Li, L., Sein, D., 2020. Evolution of Mediterranean Sea water properties under climate change scenarios in the med-CORDEX ensemble. Clim. Dyn. 54, 2135–2165. https://doi.org/10.1007/s00382-019-05105-4.

Terzić, E., Cardin, V., Le Meur, J., Dunić, N., Vodopivec, M., Vilibić, I., 2025. Unprecedented warming and salinization observed in the deep Adriatic. Limnol. Oceanogr. Lett. 10, 888–898. https://doi.org/10.1002/lol2.70051.

Vargas-Yáñez, M., Jesús García, M., Salat, J., García-Martínez, M.C., Pascual, J., Moya, F., 2008. Warming trends and decadal variability in the Western Mediterranean shelf. Glob. Planet. Chang. 63, 177–184. https://doi.org/10.1016/j.gloplacha.2007.09.001.

Von Schuckmann, K., Minière, A., Gues, F., Cuesta-Valero, F.J., Kirchengast, G., Adusumilli, S., Straneo, F., Ablain, M., Allan, R.P., Barker, P.M., Beltrami, H., Blazquez, A., Boyer, T., Cheng, L., Church, J., Desbruyeres, D., Dolman, H., Domingues, C.M., García-García, A., Giglio, D., Gilson, J.E., Gorfer, M., Haimberger, L., Hakuba, M.Z., Hendricks, S., Hosoda, S., Johnson, G.C., Killick, R., King, B., Kolodziejczyk, N., Korosov, A., Krinner, G., Kuusela, M., Landerer, F.W., Langer, M., Lavergne, T., Lawrence, I., Li, Y., Lyman, J., Marti, F., Marzeion, B., Mayer, M., MacDougall, A.H., McDougall, T., Monselesan, D.P., Nitzbon, J., Otosaka, I., Peng, J., Purkey, S., Roemmich, D., Sato, Kanako, Sato, Katsunari, Savita, A., Schweiger, A., Shepherd, A., Seneviratne, S.I., Simons, L., Slater, D.A., Slater, T., Steiner, A.K., Suga, T., Szekely, T., Thiery, W., Timmermans, M.-L., Vanderkelen, I., Wjiffels, S.E., Wu, T., Zemp, M., 2023. Heat stored in the earth system 1960–2020: where does the energy go? Earth Syst. Sci. Data 15, 1675–1709. https://doi.org/10.5194/essd-15-1675-2023.

Zhang, Y., Du, Y., Feng, M., Hobday, A.J., 2023. Vertical structures of marine heatwaves. Nat. Commun. 14, 6483. https://doi.org/10.1038/s41467-023-42219-0.